Analysis of shock tube equilibrium radiation for Earth re-entry applications

By A. M. Brandis

1. Introduction

This paper presents measurements of equilibrium radiation obtained from the NASA Ames Research Center's EAST facility and the University of Queensland's (UQ) X2 facility. Experiments have been conducted in both facilities aimed at measuring the level of radiation encountered during conditions relevant to the Orion lunar return into Earth's atmosphere. The facilities have targeted the same nominal test conditions, and spectral measurements of the emitted radiance have been obtained across a comparable wavelength range. As this paper is only an overview of the work, as opposed to the full analysis, only preliminary results have been shown with the intention that further comparisons of the spectral intensity across a wavelength range of 300 - 900 nm will be conducted. At present, a few preliminary results are shown. The methodology behind this paper is to present results from a study that will involve independently reducing the data from raw experimental counts to calibrated radiance in both facilities, and then conducting a comparison between these results. This analysis will endeavor to provide a better understanding of the uncertainty in the measurements, as well as provide a thorough comparison between the X2 and EAST results. Furthermore, this analysis will indicate whether various radiative mechanisms are due to physical processes relevant to flight, or are just facility-dependent phenomena. These phenomena include effects such as contaminating species and the level of the background continuum. Results are shown across a wavelength range of 600-830 nm. NEQAIR simulations will also be conducted for all the EAST and X2 experimental conditions and a comparison conducted. For this overview, a preliminary comparison with NEQAIR has been presented for the nominal test condition.

2. Background

With the Vision for Space Exploration, there has been renewed interest in understanding the radiation that is encountered during re-entry into Earth's atmosphere. In particular, the focus has been to consider conditions that are relevant to the Orion capsule, as part of the CEV Aerosciences Project (CAP). Because the radiation is a significant portion of the head flux, although only for a relatively short time in the trajectory, detailed simulations and experiments have been undertaken to quantify this radiation and associated uncertainties (Johnston 2008; Bose *et al.* 2008; Panesi *et al.* 2009). At present, significant differences have been found between the experimental measurements taken in the EAST facility at the NASA Ames Research Center and theoretical models, such as NEQAIR (Whiting *et al.* 1996). NEQAIR (Nonequilibrium Air Radiation) is a line-by-line radiation code computes spontaneous emission, absorption and stimulated emission due to transitions between various energy states of chemical species along a line-of-sight. Individual electronic transitions are considered for atoms and molecules, with the molecular band systems being resolved for each rotational line. For more detail about NEQAIR, the reader is referred to (Bose *et al.* 2009; Whiting *et al.* 1996). These uncertainties are therefore critical in the design of the thermal protection system (TPS).

The work presented in this paper focuses on the comparison of the experimental results from the X2 facility at UQ and the EAST facility at the NASA Ames Research Center. Because there was previously only one relevant data set for experimental data, the EAST data, this comparison should help provide an insight into the level of fidelity of the theoretical models, and any previous discrepancies that have already been identified, such as the background continuum.

3. Description of the facilities

In both facilites the heated test gas behind the shock front simulates conditions behind the bow shock on a re-entry vehicle. This enables the experiments to be performed with flow parameters, such as velocity, static pressure, and atmospheric composition close to actual flight conditions. As the tests are performed at real flight pressures, full capsule geometry must be used if it is intended to test aerodynamic features of the flow. The small region of test gas in a non-reflected shock tube makes these tests not suitable for reproducing the aerodynamic flowfield, just a small region of the flow where it is radiating. To date, there have been relatively few attempts to measure the radiative intensity of Earth entry conditions.

3.1. *EAST*

The EAST facility at NASA Ames Research Center was developed to simulate high-enthalpy, real gas phenomena encountered by hypersonic vehicles entering planetary atmospheres. It has the capability of producing superorbital shock speeds using an electric arc driver with a tube diameter of 10.16 cm (Grinstead *et al.* 2008; Bogdanoff 2008). The facility was built in the late 1960s to support research in aerothermochemistry of hypervelocity flight through Earth and planetary atmospheres. The use of an electric arc discharge as the driver mechanism permits generation of shock speeds up to 46 km/s in H_2/He atmospheres (Grinstead *et al.* 2008; Bogdanoff 2008). The region of valid test gas lies between the shock front and the contact surface that separates the driver and driven gases. The test time is defined as the axial distance between these two points divided by the local shock velocity. The characteristics of the EAST arc driver typically result in test times of 2-6 microseconds. Though short, this test time is often sufficient to capture the peak of the nonequilibrium shock radiation and the decay to equilibrium conditions.

3.2. *X2*

The experiments shown in this paper from the UQ were conducted on the X2 high-enthalpy shock tube facility (McGilvray *et al.* 2009). The most important dimension with regards to the experimental testing is the bore of the acceleration tube which is 85 mm. Previously, X2 has generally been operated as an expansion tube; however, for these experiments the facility was modified to be operated as a nonreflected shock tunnel (NRST). In this configuration, the free piston driver is used to generate a strong shock wave that passes through the secondary driver, then through the stagnant test gas in the shock tube. The secondary shock-heated driver is required in order to reach the shock velocities required for the test conditions.

4. Comparison of EAST and X2

The facility and methodology behind both X2 and EAST testing are similar, and thus they are a good source of data comparison, especially when there are several common testing conditions. However, there are two main differences between how the facilities operate and measure radiation. On EAST, the radiation is observed through a window in the side of the shock tube, whereas in X2, the radiation is observed behind the shock after it exits the tunnel. This effectively means that in EAST, the radiation passes through the shock tube boundary layer, whereas in X2, the radiation passes through an expansion fan wave structure (of which some of the flow is from the tube boundary layer) caused by the change in area as the flow propagates into the dump tank. There is the intention to conduct experiments on the X2 facility looking through the boundary layer to provide a more direct comparison with the EAST results. Because the boundary layer is less significant on the X2 facility where the measurement is taken, the effect of tube contamination from the walls of the facility may be mitigated. This could be useful factor for the comparison with EAST, as it is believed that the wall provides some contaminating species to the flow. The other relevant difference is the driver arrangement. X2 uses a free piston driver, whereas EAST uses an electric arc driven driver (Bogdanoff 2008; Bose *et al.* 2006). The advantage of the free piston driver arrangement is that it can provide longer test times.

Some issues have been identified with the calibration process of the X2 data. Thus for increased confidence in the calibration, further calibration data will be obtained on the X2 facility. At present this results in the spectra having a calibration that is less valid toward the upper and lower ends of each experimental picture. The predominant reason is that a calibration image has not been taken for all the spectrometer settings used in the experiments, and so an averaging method was implemented. With further calibration images, this averaging will not be necessary.

4.1. *Key differences in experiments*

This section will outline the differences in how each experiment is run. These differences fall under two categories:

4.1.1. *Calibration*

The source used for the absolute intensity calibration of both the X2 and EAST results is different. For the X2 calibration, a tungsten-halogen OL200M spectral calibration lamp from Optronic Laboratories is used, whereas on the EAST facility, an integrating sphere from Spheroptics with NIST (National Institute of Standards and Technology) traceable absolute radiance calibration is employed. Furthermore, both calibration sources are intended as standards for different units of absolute radiometry. The UQ lamp is calibrated as an irradiance source (meaning that the solid angle captured during an experiment needs to be calculated), while EAST uses a radiance source (thus the solid angle is intrinsic to the quoted calibration). The method for calculating the zero level is also different. In EAST a "dark" count picture is taken and subtracted from both calibration and shot data. This picture allows for the level of counts on each pixel to be found when there is no light source illuminating the slit. This method assumes that there is no stray light entering the slit during the experiment, whereas X2 has the advantage of being able to correct for any stray light that has entered spectrometer, but has the disadvantage of assuming all sources of background have no spatial dependence on the pixel array.

The effect of non-reciprocity is also addressed differently in the two facilities. On

EAST, different exposure times for the calibration and the experiment are used and the experimental exposures can be several orders of magnitude smaller than those for calibration. This is done so the level of the counts between experiment and calibration are approximately the same. A correction factor is then employed to correct for the effect of non-reciprocity. In X2 the same exposure time is used for the experimental and calibration image and no reciprocity correction is needed. However, because the calibration picture has a small exposure time, the number of counts can be very low, especially in the UV region of the spectrum. Therefore, UQ relies on linearity of the pixel counts versus intensity and accepts an increased level of uncertainty on the UV calibration, while EAST relies on the linearity of pixel counts versus intensity and on the reciprocity function being constant and well known.

Another difference regarding the calibration is the way in which the optical arrangement is configured between the two different procedures. On the EAST facility, the integrating sphere is placed at a location representative of the center-line of the tunnel, and the emitted light is captured by exactly the same optical arrangement as that used in the experiment. However, this approach is not very practical in the X2 facility because the source is an irradiance, rather than radiance source. Furthermore, the use of intervening optics would reduce the counts such that a reciprocity correction may be required. The effect of the intervening optics then has to be taken into account, e.g., optical magnification, losses due to mirrors and windows. The counts are still low in the UV using this method because the calibration lamp had to be placed approximately 4 m back from the center-line of the tunnel in order to match the F/# of the collection optics and to confirm that all light emitted by the lamp going through the virtual pixels in the test section was being captured by the spectrometer.

4.1.2. *Experimentation*

Owing to the possibility of many different experimental settings and optical arrangements, a simple comparison of spectra from EAST and X2 may not be relevant. There are effects such as different exposure times, different slit widths, different resolutions in wavelength and averaging over assumed equilibrium areas of the flow. It is the aim of this paper to select not only experiments for comparison with similar testing conditions, but also similar experimental settings. Furthermore, several analyses will be undertaken with integrated spectral features, thus discounting effects of different slit widths and wavelength resolutions. CFD (Computational Fluid Dynamics) analyses are also required for X2 to determine the quality of the flow and the effect of the expansion fan at the exit of the tunnel. This analysis would help determine the length of the test time, and, more importantly, evaluate the width of the radiating gas that is emitting the light collected by the spectrometer. The width of the radiating gas is expected to vary with the distance out of the tube. The CFD analysis should help to quantify this effect.

5. Experimental results

5.1. *Equilibrium condition assumption*

A critical aspect of these shock tunnel experiments is whether or not the flow has reached equilibrium conditions. Owing to the short time-scales and complex flow in shock tunnels, this condition is neither guaranteed nor easily quantifiable. An analysis was undertaken to assess the level of equilibrium that was achieved in the EAST facility. It is also planned that this analysis will be extended to the X2 results in the future. The analysis involves

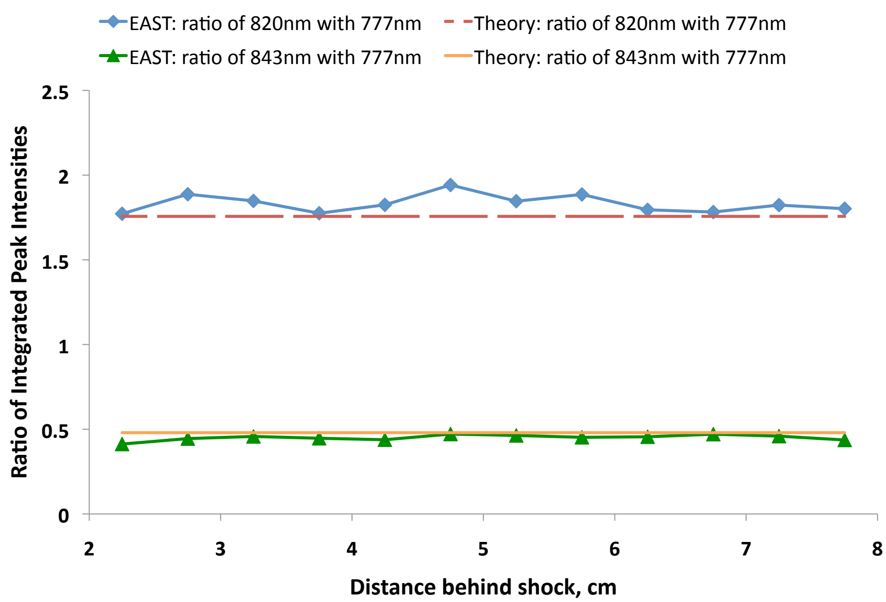

FIGURE 1. Comparison of the ratio of the integrated intensities of the 820 nm, 843 nm and 777 nm with theory at different axial positions behind the shock.

looking at the evolution of the ratios of various integrated line intensities at distances behind the shock where equilibrium is thought to exist. Figure 1 shows how the ratio of both the integrated line intensities of 820 nm (Nitrogen) and 843 nm (Nitrogen) with 777 nm (Oxygen) behind the shock. The experimental values are then compared with theoretical values. Ratios have been used as an equilibrium indicator, as opposed to an absolute measurement, to remove quantities from the analysis that maybe changing with time, such as flow density and pressure. As figure 1 shows, the agreement between the EAST data and theory is very good, and the ratio is very constant with distance behind the shock, indicating that at least local equilibrium has been reached. It is intended that this analysis will be extended to several other lines, including lines that are in different regions of the spectrum.

5.2. *Analysis and comparison*

One issue for the presentation of the experimental data for comparison purposes is the units to be used for the radiative intensity. When the intensity is calibrated, the units are given as an absolute spectral radiance, $\mathrm{W/cm^2/\mu m/sr}$. This represents the radiance from a two-dimensional surface such as the imaging window or edge of the shock wave. This radiance is equivalent to the volumetric radiance in the shock integrated over the line of sight of the collection optics. However, in terms of comparing the EAST and X2 results, these units may not be directly compared because the tunnels have different diameters. Furthermore, the core-flow on the X2 facility is reduced even further owing to the expansion fan process. Therefore, for an adequate comparison, the radiative intensities need to be expressed in terms of volumetric units, i.e., $\mathrm{W/cm^3/\mu m/sr}$. To make this conversion, the width of the radiating gas over which the measurement was integrated needs to be known. As on the EAST facility the measurement is taken while inside the shock tube, this width can be said to be the width of the tube. This means that the

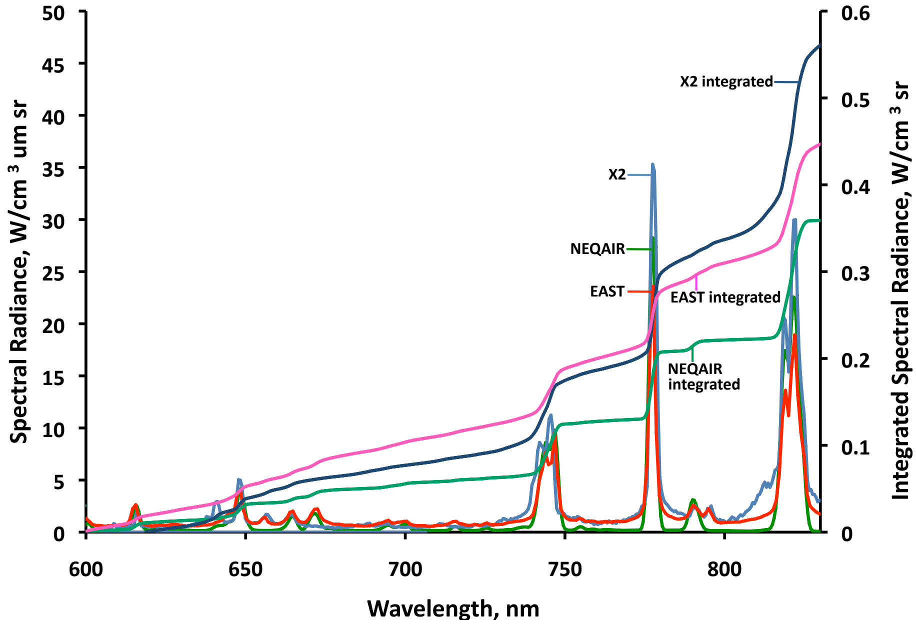

FIGURE 2. Comparison of EAST and X2 at 10.0 km/s, 26.6 Pa in air.

boundary layer has been assumed to have a negligible thickness. For comparison, a core width of X2 has been assumed. In a previous CFD analysis it was estimated that the minimum core width was 60 mm at the nonequilibrium peak of radiative intensity. So for this analysis, this is assumed to be the lower limit. The upper limit is the width of the tunnel, which is 85 mm. Therefore, for this preliminary analysis, the core width has been assumed to be simply the average of the upper and lower limits, 72.5 mm. This value therefore has an uncertainty bound of ± 17%, and should be considered as a very basic estimate of core flow until further CFD results have been obtained. It should also be noted that the wavelength calibration of the X2 data had to be shifted to align with known spectral peaks. This transformation was required owing to a slight error in the wavelength calibration of the grating.

Figure 2 shows that in the "Red" range of the spectrum, the agreement between the EAST and X2 results is generally very good. Due to the averaging used in the current calibration process, the camera response function against wavelength is not completely taken into account in the calibration image on the X2 facility: one "smoothed" calibration vector was constructed over the spectral range of the spectrometer, rather than individual calibration vectors for each spectrometer setting. Hence, the calibration from approximately 800 nm onward becomes less and less accurate. With this averaged calibration vector, the integrated radiative intensity showed excellent agreement up until 800 nm, within 15%. However, from 800 nm the disagreement becomes larger and larger. By 900 nm, X2 shows a 70% larger radiative intensity than that seen on EAST. It is expected that with more calibration images from the X2 experimental set-up, these measurements will come into closer agreement. The comparison in figure 2 has been shown only up to 830 nm due to questions regarding the validity of the calibration above this wavelength.

In this range, the agreement between the two spectra is good, within 25%. It is in-

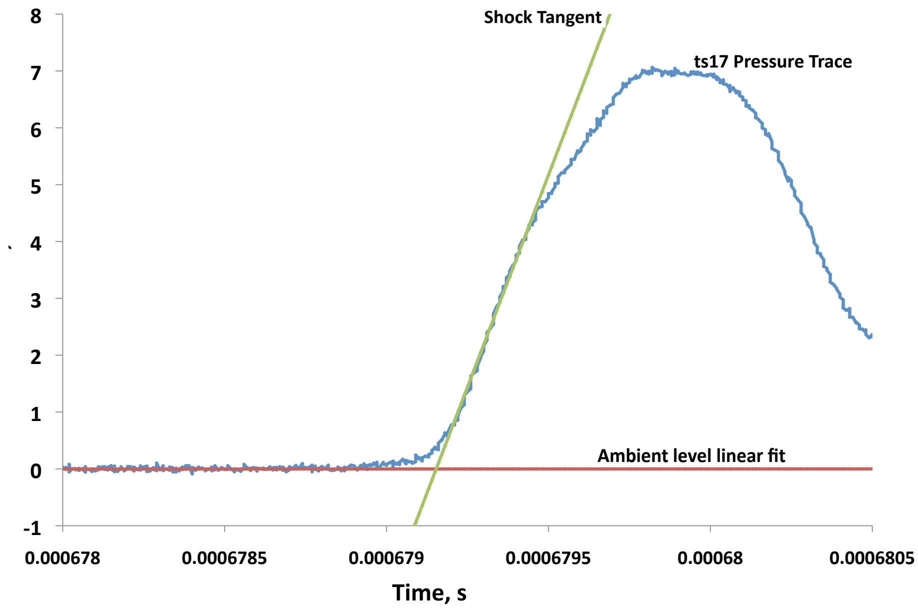

FIGURE 3. The tangent method for calculating shock speed off a pressure trace.

tended to compare several more spectra in the future, to see if this agreement is found across several other conditions. Spectrally, the results agree very well, with only minor differences. The EAST data show a small spectral feature at 670.6 nm which is not seen on X2, while X2 shows a small spectral feature at 640.2 nm not seen on the EAST data. The first of these features is predicted by NEQAIR and is attributable to atomic N 3p-4d transition. The latter feature may also be assigned to atomic N 3p-4d transition, but does not match the NEQAIR prediction. Note that the contribution of the background continuum is very similar between the two facilities. Note also that to do a full comparison between the two facilities, high-fidelity CFD is required to quantify the flow structure in both facilities. This is an area that is currently being investigated. Furthermore, at present only very preliminary results have been obtained from the UV comparison and thus are not presented.

5.3. *Shock speed sensitivity*

Because of the nature of the flow under investigation during these experimental campaigns, the sensitivity with respect to the shock speed is very high. Thus a very accurate measurement of the shock speed is required. The magnitude of the atomic radiation lines is highly influenced by the shock speed. These atomic lines being the predominant source of radiation in the IR range of the spectrum. For example, a change of shock speed from 9.6 km/s to 10.8 km/s corresponds to an order-of-magnitude increase in radiation.

The shock speed on EAST is measured through a series of pressure transducers that measure the time of arrival (ToA) of the shock wave. The accuracy to which the shock speed can be measured on EAST varies between 0.5 to 1.0%, whereas on the X2 facility the error in the shock speed is higher, in the order of 2%. This importance of accurately knowing the shock speed necessitates a new method for calculating the shock speed. The process involves fitting the zero level and the shock tangent with linear fits. The point in time at which these two lines cross is then deemed to be the time of arrival, see figure 3. This process has so far proved to be more self-consistent and shows less variation from transducer to transducer. It is also intended that an uncertainty quantification analysis will be conducted on the EAST shock speed calculations, and the resulting radiative intensities. The level of noise associated with the two tangent fits can provide a probability density function (PDF) of the shock speed variation. This variation can then be used as an input into NEQAIR and a PDF of the radiative intensity based on the uncertainty in shock speed can be calculated.

6. Future work

Many more comparisons of the X2 and EAST results are likely at different pressures and shock speeds. Furthermore, a more in-depth analysis of comparing various line intensities at different shock speeds will be conducted so that a distribution of the data can be analyzed. It is also hoped that more calibration images will be taken with the X2 configuration for all the arrangements used in the testing campaign to achieve an increased confidence in the data reduction process. A thorough uncertainty quantification analysis is also planned on both experimental set-ups.

Acknowledgments

The author would like to thank the following people: Nagi Mansour, Parviz Moin and Gianluca Iaccarino for all their efforts and support for my Postdoctoral Research Fellow position at Stanford University and NASA Ames Research Center; Brett Cruden, Deepak Bose, Dinesh Prabhu, Ramon Martinez and Hai Le for the experimental data and NEQAIR analysis from NASA Ames Research Center's EAST facility; and Matthew McGilvray, Richard Morgan and Tim McIntyre for the experimental data from the University of Queensland's X2 facility.

REFERENCES

Bogdanoff, D. W. 2008 Shock tube experiments for Earth and Mars entry conditions. In *Von Karmen Institute Lecture Series*.

Bose, D., McCorkle, E., Bogdanoff, D. W. & Allen Jr., G. 2009 Comparisons of air radiation model with shock tube measurements. In *47th AIAA Aerospace Sciences Meeting*. Orlando, Florida, AIAA Paper 2009-1030.

Bose, D., McCorkle, E., Thompson, C., Bogdanoff, D. W., Prabhu, D. & Allen Jr., G. 2008 Analysis and model validation of shock layer radiation in air. In *46th AIAA Aerospaces Sciences Meeting and Exhibit*. Reno, Nevada, AIAA Paper 2008-1246.

Bose, D., Wright, M., Bogdanoff, D., Raiche, G. & Allen Jr, G. 2006 Modelling and experimental validation of CN radiation behind a strong shock wave. *Journal of Thermophysics and Heat Transfer* **20** (2), 220–230.

Grinstead, J., Wilder, M., Wright, M., Bogdanoff, D., Allen Jr., G., Dang, K. & Forrest, M. 2008 Shock radiation measurements for Mars aerocapture radiative heating analysis. In *46th AIAA Aerospace Sciences Meeting and Exhibit*. Reno, Nevada, AIAA Paper 2008-1244.

Johnston, C. 2008 Nonequilibrium shock-layer radiative heating for Earth and Titan entry. In *46th AIAA Aerospace Sciences Meeting*. Reno, NV, AIAA Paper 2008-1245.

McGilvray, M., Morgan, R. & McIntyre, T. 2009 Shock tube measurements in the X2 facility of radiation from CEV re-entry conditions: Initial report for 0.2 torr testing. *Tech. Rep.* 1.1. University of Queensland.

Panesi, M., Magin, T., Bourdon, A., Bultel, A. & Chazot, O. 2009 Analysis of the Fire II flight experiment by means of a collisional radiative model. *Journal of Thermophysics and Heat Transfer* (Accepted for publication).

Whiting, E., Yen, L., Arnold, J. & Paterson, J. 1996 NEQAIR96: Nonequilibrium and equilibrium radiative transport and spectra program user's manual. *Tech. Rep.* NASA RP-1389. NASA.